Journal of Sound and Vibration (2002) **255**(2), 229–242
doi:10.1006/jsvi.2001.4152, available online at http://www.idealibrary.com on IDEAL®

A SIMPLE MODEL TO ESTIMATE THE IMPACT FORCE INDUCED BY PISTON SLAP

S.-H. Cho, S.-T. Ahn and Y.-H. Kim

Center for Noise and Vibration Control (NOVIC), Department of Mechanical Engineering, Korea Advanced Institute of Science and Technology (KAIST), Science Town, Daejon 305-701, Korea.
E-mail: shcho617@cais.kaist.ac.kr; sangtaea@engin.umich.edu; yhkim@mail.kaist.ac.kr

(*Received* 2 *April* 2001, *and in final form* 28 *September* 2001)

The dynamics of piston's secondary motion (lateral and rotational motion) across the clearance between piston and cylinder inner wall of reciprocating machines are analyzed. This paper presents an analytical model, which can predict the impact forces and vibratory response of engine block surface induced by the piston slap of an internal combustion engine. A piston is modelled on a three-degree-of-freedom system to represent its planar motion. When slap occurs, the impact point between piston skirt and cylinder inner wall is modelled on a two-degree-of-freedom vibratory system. The equivalent parameters such as mass, spring constant, and damping constant of piston and cylinder inner wall are estimated by using measured (driving) point mobility. Those parameters are used to calculate the impact force and for estimating the vibration level of engine block surfaces. The predicted results are compared with experimental results to verify the model.
© 2002 Elsevier Science Ltd. All rights reserved.

1. INTRODUCTION

One of the major sources of noise and vibration in an internal combustion engine is the impact between piston and cylinder wall. The crank-slider mechanism of an internal combustion engine has very small clearance between piston and cylinder inner wall. The clearance is very small but large enough to induce the piston's secondary motion periodically and finally generates unwanted sound and vibration (Figure 1). This secondary motion across the clearance between piston and cylinder inner wall is caused by the side thrust force that changes its direction depending on its position (Figure 2). This side thrust force is induced by the connecting rod. As a result, the piston moves from one side to opposite side in the cylinder. Then eventually, the piston collides against the cylinder inner wall (Figure 2). These impact phenomena are called "piston slap".

There have been many attempts to model or estimate the impact forces and the side thrust force. These are a function of inertia force of piston and connecting rod and explosive force in internal combustion engine [1–4]. There are also studies on the dynamics of planar crank-slider mechanism in order to investigate the influence of the clearance gap size, bearing friction, and crank speed on the response of the system; for example, see references [5, 6]. Finite Element Method (FEM) has been also applied in order to analyze the impact force [7]. However, the models as well as FEM are not satisfactory to estimate the impact forces. This is because the basic mechanism associated with the piston slap is complicately related to the mechanical elements of engine block.

We need, therefore, to consider the piston slap as much in detail as possible to improve the quality of prediction. This paper describes how we model the dynamics of piston slap

0022-460X/02/$35.00 © 2002 Elsevier Science Ltd. All rights reserved.

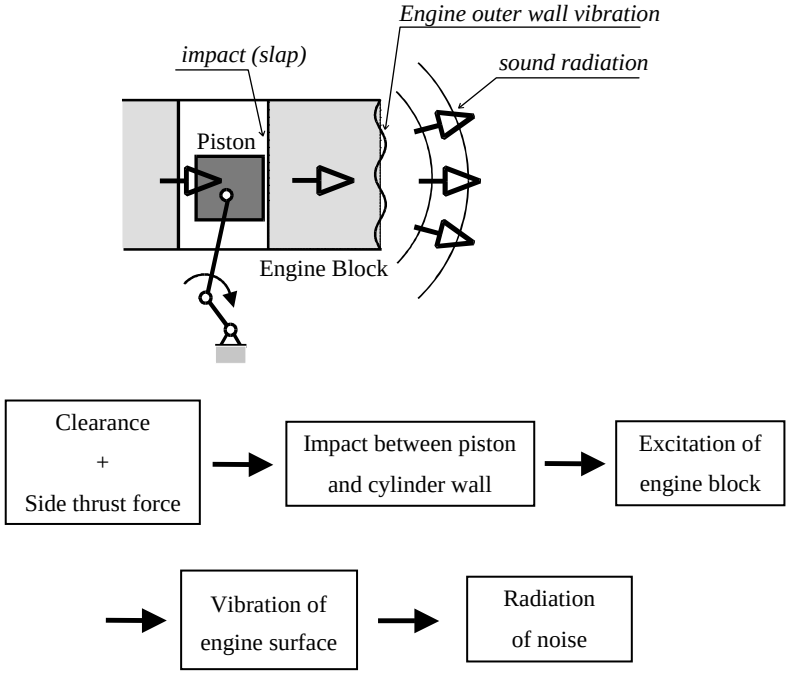

Figure 1. Schematic diagram of generation of engine noise/vibration related to piston slap.

induced vibration. Based on the model, we estimated the impact forces of piston in cylinder. The engine block surface vibration response is predicted by convoluting the impact forces with measured impulse responses between the cylinder inner walls and engine block outer surfaces. Experimental verification on the predicted response has been also performed by experiment using a commercial 4-cylinder diesel engine. The errors in estimating the impact force and vibration response at engine block surface are also studied.

2. MODEL DESCRIPTIONS AND EQUATIONS OF MOTION

2.1. A MODEL AND EQUATIONS OF MOTION OF A PISTON

We propose a two-dimensional lumped parameter model as shown in Figure 3. This figure describes the piston motion in translation along the x, and y-axis and the rotation around the piston pin axis. We neglected the motion in z-axis and angular motion other than the piston pin axis. This is simply because those effects on the impact are negligible compared with what we propose to consider.

The piston impact on the cylinder inner wall occurs at the upper and lower ends of the piston skirt. The piston skirt stiffness can be modelled on a linear spring located on those impact points. The oil film between the piston skirt and the cylinder inner wall would experience reaction forces induced by the vertical piston movement and the lateral piston movement. This can be approximately modelled on a viscous damping based on Reynold's equation [8].

The piston moves in three directions (vertical, lateral, and rotational directions). The motions in both lateral and rotational directions are called piston's secondary motion. If we

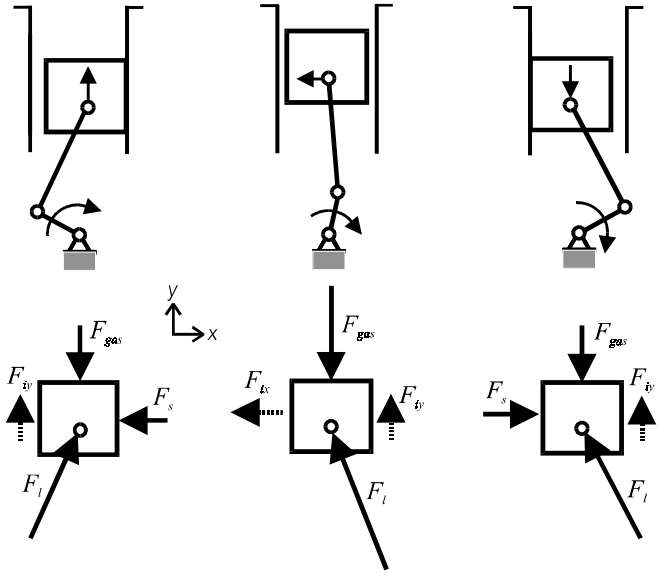

(a) before TDC (b) at TDC (c) after TDC

F_{gas} : gas force by combustion
F_l : reacting force by connecting rod
F_S : reacting force by cylinder inner wall
F_{ix} : x -direction inertia force
F_{iy} : y -direction inertia force
TDC : top dead center

Figure 2. Forces and geometrical configuration of piston slap.

define the piston position co-ordinates (x_p, y_p, θ_p) at the piston pin position (P in Figures 3 and 4), the inertia force F_{ix} in the horizontal direction (x-axis), the inertia force F_{iy} in vertical direction (y direction), and the inertia force $M_{i\theta}$ in the rotational direction (θ-axis) are readily obtained. That is

$$F_{ix} = m_p \ddot{x}_{COG} = m_p\{\ddot{x}_p + s(\ddot{\theta}_p \cos(\gamma + \theta_p) - \dot{\theta}_p^2 \sin(\gamma + \theta_p))\}, \tag{1}$$

$$F_{iy} = m_p \ddot{y}_{COG} = m_p\{\ddot{y}_p - s(\ddot{\theta}_p \sin(\gamma + \theta_p) + \dot{\theta}_p^2 \cos(\gamma + \theta_p))\}, \tag{2}$$

$$M_{i\theta} = I_p \ddot{\theta}_{COG} = I_p \ddot{\theta}_p, \tag{3}$$

where m_p, I_p are mass and mass moment of inertia of piston respectively. $s = \sqrt{l_x^2 + l_y^2}$ is piston pin offset distance. $\gamma = \cos^{-1}(l_y/\sqrt{l_x^2 + l_y^2})$ is piston pin offset angle (Figure 3). Considering the applied external forces, we can obtain the equations of motion that describes the response of piston subjected to the external forces. Those are

$$m_p\{\ddot{x}_p + s(\ddot{\theta}_p \cos(\gamma + \theta_p) - \dot{\theta}_p^2 \sin(\gamma + \theta_p))\} = A_x + F_A + F_B - F_C - F_D, \tag{4}$$

$$m_p\{\ddot{y}_p - s(\ddot{\theta}_p \sin(\gamma + \theta_p) + \dot{\theta}_p^2 \cos(\gamma + \theta_p))\} = -A_y - F_{gas} - F_{fric} - m_p g, \tag{5}$$

$$\begin{aligned} I_p \ddot{\theta}_p = {} & F_{gas}(x_{BO} - x_p) + F_A l_{yA} - F_B l_{yB} - F_C l_{yC} + F_D l_{yD} \\ & + m_p g \cdot s \sin(\gamma + \theta_p) - T_{fric} + m_p \ddot{x}_p l_y - m_p \ddot{y}_p l_x, \end{aligned} \tag{6}$$

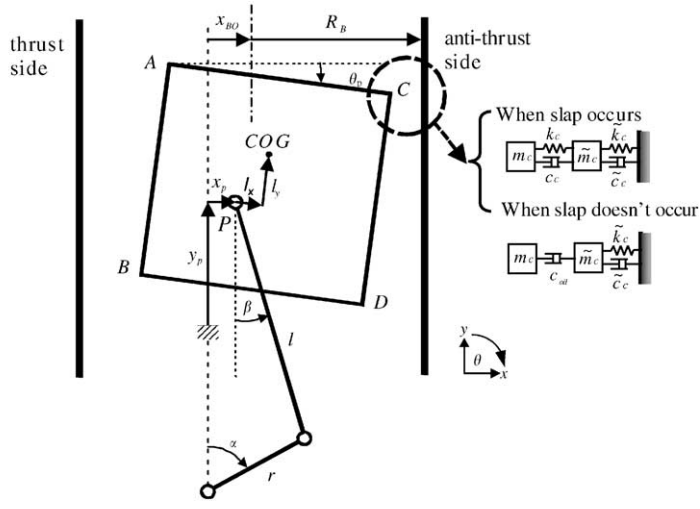

P	: piston pin position
COG	: center of gravity of piston
A,B,C,D	: the impact points(piston skirt)
l	: length of connecting rod
r	: crank radius
x_p	: x-directional position of piston pin
y_p	: y-directional position of piston pin
R_B	: bore radius
x_{BO}	: bore offset

Figure 3. Model of the piston and the cylinder inner wall.

where the F_A, F_B, F_C, F_D are the impact forces exerted on the piston skirts A, B, C, D, respectively. The $F_{gas}, F_{fric}, T_{fric}, A_x, A_y$ are explosive force in the cylinder, friction force on piston wall, friction torque exerted on the piston pin, lateral and vertical direction reaction forces transmitted from connecting rod respectively. $l_{yA}, l_{yB}, l_{yC}, l_{yD}$ are distances along the y-axis between piston pin position and piston skirt position A, B, C, D, respectively. Especially, side thrust force A_x is the driving force, which causes the piston's secondary motion (Figure 4).

In the equations of motion (equations (4)–(6)), the variables that we want to solve are accelerations ($\ddot{x}_{COG}, \ddot{y}_{COG}, \ddot{\theta}_{COG}$) of the center of gravity of the piston in three directions, the impact forces (F_A, F_B, F_C, F_D) exerted on the piston skirts, and lateral and vertical direction reaction forces (A_x, A_y) transmitted from the connecting rod. We have three equations of motion but have nine unknown variables. Hence, six supplementary equations of motion or constraints must be needed. It is noteworthy that translational accelerations ($\ddot{x}_{COG}, \ddot{y}_{COG}$) of the center of gravity of the piston are not independent unknown variables but a function of $\theta_p, \dot{\theta}_p$ and $\ddot{\theta}_p$. In other words, we can find the translational position, velocity, and acceleration of the piston from kinematics of crank-slider mechanism as shown in Figure 3. Therefore, we need four supplementary equations of motion. Those equations can be obtained from the proposed model that describes the mechanism at collision points. Next section addresses the model.

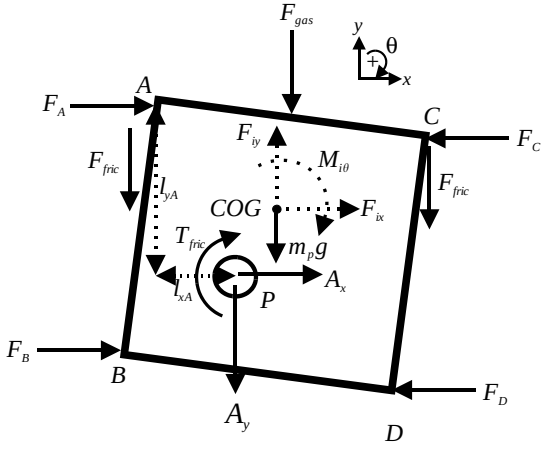

F_{gas}	: gas force
F_A, F_B, F_C, F_D	: the impact force when slap occurs
A_x, A_y	: reacting force by connecting rod
F_{fric}	: friction force between piston and cylinder inner wall
T_{fric}	: friction torque between piston and piston pin
F_{ix}	: x-direction inertia force of piston
F_{iy}	: y-direction inertia force of piston
$M_{i\theta}$	: θ-direction inertia force of piston

Figure 4. Free body diagram of the piston.

2.2. A MODAL OF COLLISION POINTS AND SUPPLEMENTALY EQUATIONS OF MOTION

2.2.1. *Basic concept of point mobility*

Mobility is defined as the ratio of a velocity to a force. Mobility between different input and output points is called "transfer mobility", and mobility at a point is often called "(driving) point mobility". This measure is sometimes used to estimate the mass, spring constant, and damping constant of lumped parameter system [9]. The point mobility essentially expresses the relation between an excited force and a response (velocity). This provides us to express the relations between the impact force and the responses of the piston skirt and the cylinder inner wall. If the responses of the piston skirt and cylinder inner wall at a certain point are known or can be measured, the corresponding impact force can be deduced if we know the point mobility. This motivates to model the point mobility.

Figure 5 shows the basic concept of the point mobility. For simplicity, let us examine first that of a fixed–free bar. In this case, the point mobility can be derived as

$$M = \mathrm{j}\frac{c}{EA}\tan kl, \tag{7}$$

where E, A, ρ, l are Young's modulus, cross–section area, density, and length of bar, respectively, c is the speed of wave propagation, and k the wave number [10]. As Figure 5 shows, the bar behaves like a linear spring in the frequency range below the first resonance

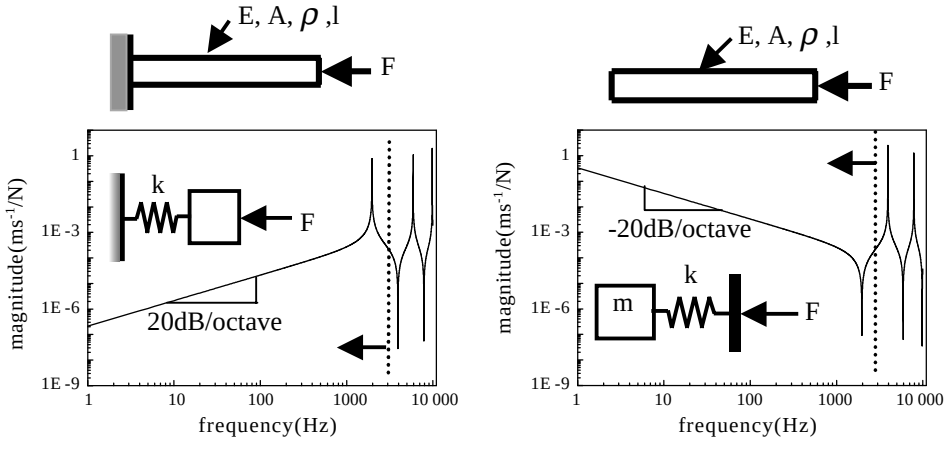

(a) In the case of fixed-free bar (b) In the case of free-free bar

Figure 5. Point mobilities of bar and equivalent lumped parameter system in frequency range of interest.

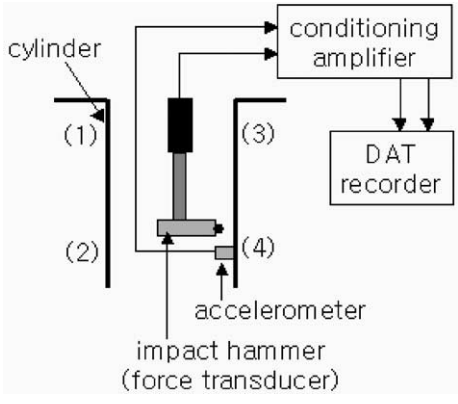

Figure 6. Experimental set-up in order to measure the driving point mobilities at four different impact points (1)–(4).

peak. It is notewothy that point mobility inceases 20 dB/octave (Figure 5(a)). This tells us that the bar can be modelled on one-degree-of-freedom vibratory system in the frequency range below the first resonance peak.

On the other hand, if a bar has free-free boundary condition, then the point mobility is [10]

$$M = \mathrm{j}\,\frac{c}{EA}\cot kl. \tag{8}$$

Equation (8) indicates that the point mobility decreases 20 dB/octave in the frequency range below the first anti-resonance peak. Therefore, again the bar can be modelled on one-degree-of-freedom vibratory system in the frequency range below the first anti-resonance peak. The system is excited through the base (Figure 5(b)).

These two simple models suggest that we could express the mechanical behavior of the system that is involved in piston slap in terms of these two models. The measured point

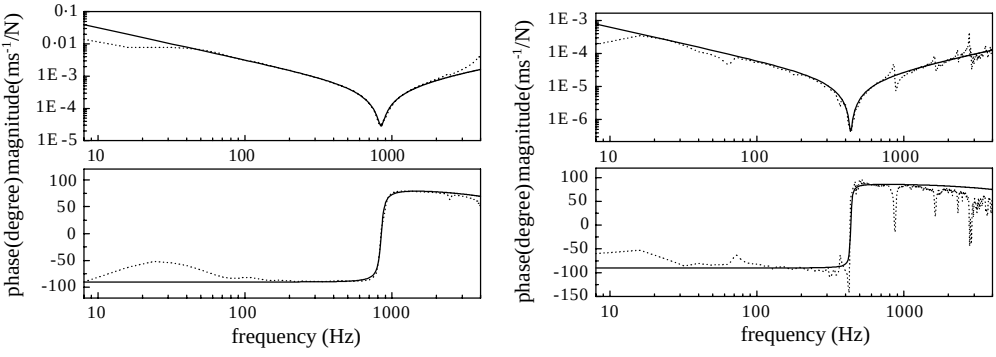

(a) at piston skirts (b) at cylinder inner walls

Figure 7. Point mobilities of piston skirt and cylinder inner wall (——, estimated curve by using equation (9); ----, experimental curve measured in freely supported condition).

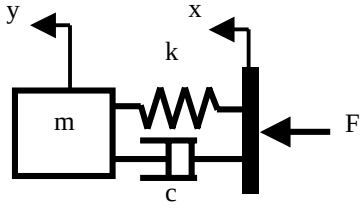

Figure 8. Base-excited one-degree-of-freedom vibratory system in freely suspended condition. This model is used to estimate the equivalent parameters using in simulation.

mobility (Figure 7), that expresses the relation between impact force and the vibration velocity of a piston or a cylinder inner wall, can be expressed and explained by using the first model (Figure 5(b)). This is because measured point mobilities show the anti-resonance peak first (Figure 7). It means that each collision point can be considered as one-degree-of-freedom vibratory system like the second model (Figure 5(b)). The assumption behind the using of these models is that the excitation frequencies must be in the region where the first mode dominates (Figure 5).

2.2.2. *Point mobility of piston skirt and cylinder inner wall*

The measured point mobilities of piston skirt and cylinder inner wall are shown in Figure 7 as dotted line. This indicates that this point mobility resembles that of free-free bar (Figure 5(b)). If we include damping effect on this model, then the point mobility model can be written as

$$M(\mathrm{j}\omega) = \frac{V(\mathrm{j}\omega)}{F(\mathrm{j}\omega)} = -\frac{\mathrm{j}\omega((k - m\omega^2) + \mathrm{j}c\omega)}{m\omega^2(k + \mathrm{j}c\omega)}, \tag{9}$$

where M, V, F are the point mobility, velocity, and force respectively (Figure 8). Equation (9) represents the thoeretical point mobility in the case of a base-excited one-degree-of-freedom vibratory system.

In the frequency range below anti-resonance frequency ω_a $(= k/m)$, the point mobility equation (9) can be approximated as $M(\mathrm{j}\omega) \cong -\mathrm{j}/m\omega$. Therefore, the magnitude $|M(\mathrm{j}\omega)|$ of the point mobility in this frequency range decreases 20 dB/octave as frequency increases

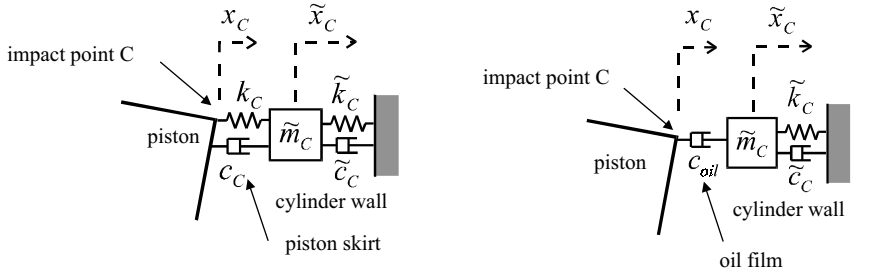

(a) When slap occurs (b) When slap doesn't occur

Figure 9. Model of the impact point (in the case of skirt C). Subscripts "C" and "oil" represent the piston skirt C and oil film, respectively, and tilde " $\sim$ " is used for cylinder wall parameters.

and the level is mainly determined by mass m. In the frequency range above anti-resonance frequency ω_a, the point mobility equation (9) can be $M(\mathrm{j}\omega) \cong -\mathrm{j}\omega/k$ approximately. In this case, the magnitude $|M(\mathrm{j}\omega)|$ of the point mobility in this frequency range increases 20 dB/octave as frequency increases. The level is mainly determined by spring constant k.

This model gives us the equivalent parameters such as mass m, spring constant k, and damping constant c. A curve fitting equation (9) with the measured driving point mobility has to be done for this purpose. Figure 6 shows the schematics of the experimental set up that was used for obtaining driving point mobilities at four different points. The driving point mobility was measured by using one accelerometer and one force transducer as shown in Figure 6. Figure 7 shows how the measured point mobilities well follow predicted ones obtained by using the parameters (Appendices A and B). The point mobilities of the cylinder inner wall; the measured point mobility and predicted one in the frequency range above about 500 Hz do not agree well. This deviation could produce some error in prediction of the impact forces above about 500 Hz.

2.2.3. *Equations of motion at collision points*

Because the position of a piston pin differs from the center of gravity of a piston, moment about the piston pin must be generated by the side thrust force, which is a lateral component of the force induced by the connecting rod. Therefore, rotational motion of the piston is unavoidable. When a piston collides against the inner wall of a cylinder, piston skirt contacts firstly. And the side thrust force exerts on the piston continuously, then the lateral area of the piston contacts with the cylinder inner wall. The proposed model considers the collision points as equivalent vibratory systems in the sense of driving point mobility. At the piston skirts, supplementary equations of motion now can be derived as follows.

$$k_i(\tilde{x}_i - x_i) + c_i(\dot{\tilde{x}}_i - \dot{x}_i) = F_i\,, \qquad c_{oil}(\dot{\tilde{x}}_i - \dot{x}_i) = F_i\,, \tag{10, 11}$$

where subscript i represents the name of piston skirts A, B, C, D. Equation (10) describes the dynamics when slap occurs, and equation (11) is for one when slap doesnot occur at each piston skirt (Figure 9). The variables with the symbol " $\sim$" represent the ones related to the cylinder inner wall. c_{oil} is the equivalent damping constant, which is deduced by Reynold's equation [8]. However, there are new unknown variables in equation (10) and (11). These are displacement ($\tilde{x}_i$) and velocity ($\dot{\tilde{x}}_i$) of the cylinder inner wall. In order to solve equations

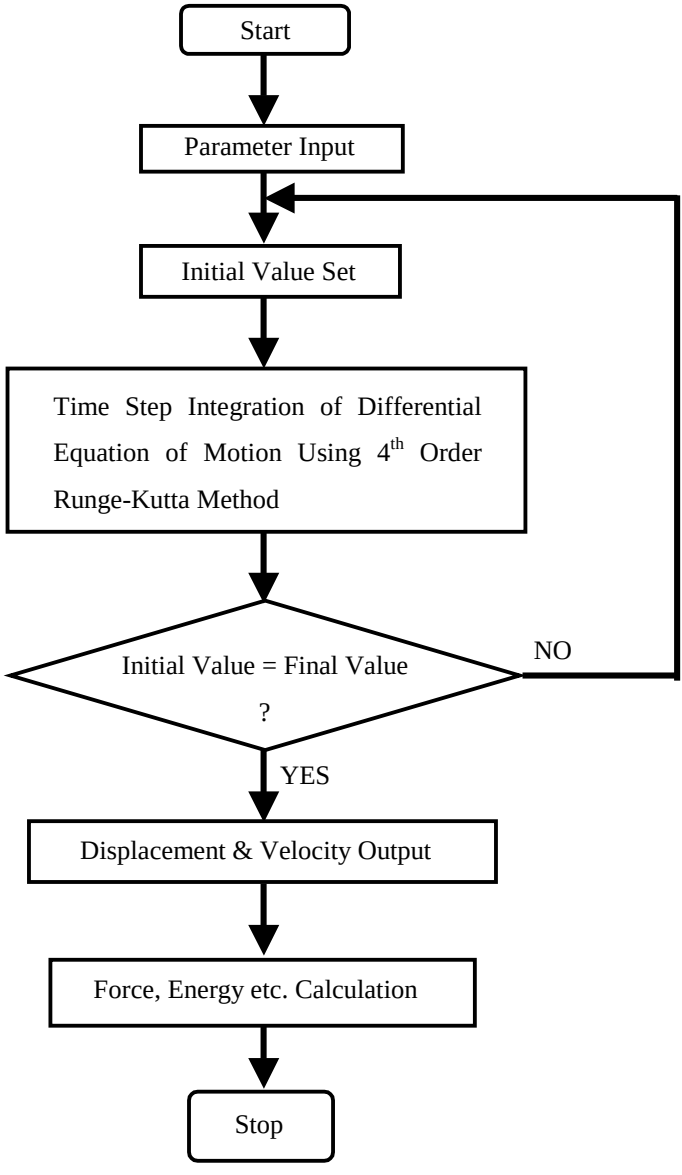

Figure 10. Flow chart for computer simulation to calculate the piston's secondary motion, impact forces in slap, piston's transverse kinetic energy and so on. Input parameters are r.p.m., connecting rod length, crank radius, piston's mass property, clearance, piston pin offset, and oil viscosity. Initial values are lateral and rotational position and velocity of piston.

(10) and (11), additional equations of motion are needed. We can easily derive the new equations of motion from the collision points at the cylinder inner walls. The new supplementary equations of motion are derived as

$$\tilde{m}_i \ddot{\tilde{x}}_i + \tilde{c}_i \dot{\tilde{x}}_i + \tilde{k}_i \tilde{x}_i = F_i, \tag{12}$$

where subscript i also represents the name of piston skirts A, B, C, D.

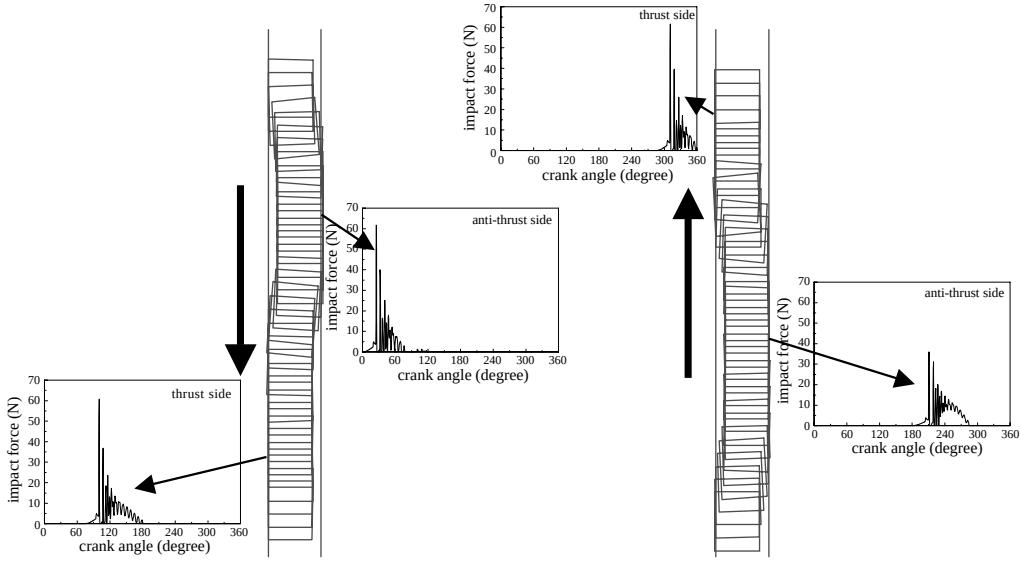

Figure 11. Animation of piston's secondary motion in 500 r.p.m. motoring condition and the impact forces when slap occurs. (In fact, this figure is exaggerated for visualization.)

3. NUMERICAL SIMULATION AND EXPERIMENTAL VERIFICATION

As stated in section 2, the independent variables related to piston's secondary motion are $\ddot{\theta}_p$, A_x, and A_y in equations (4)–(6). So, we can rewrite equations (4)–(6) as follows:

$$\begin{bmatrix} 1 & 0 & -m_p s\cos(\gamma+\theta_p) \\ 0 & 1 & -m_p s\sin(\gamma+\theta_p) \\ 0 & 0 & I_p \end{bmatrix} \begin{bmatrix} A_x \\ A_y \\ \ddot{\theta}_p \end{bmatrix} = \begin{bmatrix} -\sum F_x + m_p\ddot{x}_p - m_p\dot{\theta}_p^2 s\sin(\gamma+\theta_p) \\ -\sum F_y - m_p\ddot{y}_p + m_p\dot{\theta}_p s\cos(\gamma+\theta_p) \\ \sum M_\theta + m_p\ddot{x}_p l_y - m_p\ddot{y}_p l_x \end{bmatrix} \tag{13}$$

where

$$\sum F_x = -F_A - F_B + F_C + F_D$$

$$\sum F_y = F_{gas} + F_{fric} + m_p g$$

$$\sum M_\theta = F_{\text{gas}}(x_{BO} - x_p) + F_A l_{yA} - F_B l_{yB} - F_C l_{yC} + F_D l_{yD} - T_{fric} + m_p g \cdot s\sin(\gamma+\theta_p).$$

The right side of equation (13) is composed of external forces or moments and translational inertia forces of the piston. $\sum F_x$ represents the sum of impact forces. These are calculated from equations (10)–(12) at each piston skirt. Once impact forces are calculated, equation (13) can be readily solved by using numerical integration such as the fourth order Runge–Kutta method [11]. Once after calculating θ_p, $\dot{\theta}_p$and $\ddot{\theta}_p$, we can calculate the position ($\ddot{x}_{COG}$, $\ddot{y}_{COG}$) of the piston. Figure 10 is the simulation flow chart. Because of using numerical integration, initial values are very crucial. But we do not know the exact initial values. Because piston slap phenomena are repeated inevitably along the cycle, final values

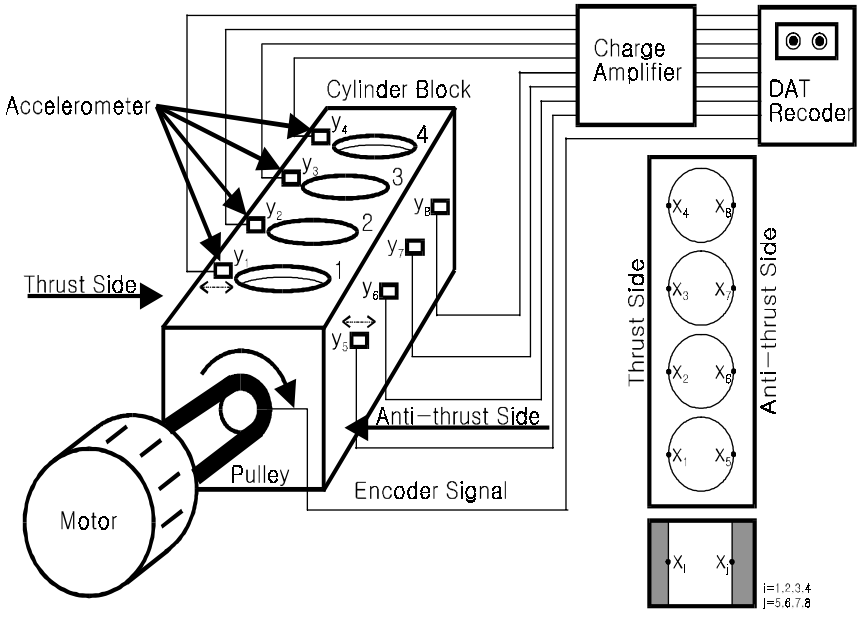

Figure 12. Experimental set-up and measuring points. Measuring point y is located on engine block surfaces and the impact point x on cylinder inner walls.

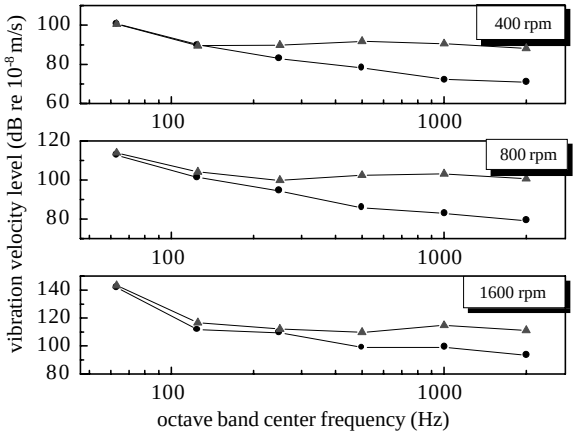

Figure 13. Comparison between estimated (△) and measured (○) vibration velocity level at engine block surface in three selected motoring conditions.

after one cycle must be same as initial values. If we examine whether final values are same as initial values or not, we can solve equations (4)–(6) and equations (10)–(12) successfully.

In this paper, results of the numerical simulation are compared with measured vibration velocity level at engine block surfaces in order to verify the proposed model. All vibration velocity level is averaged in time (1-cycle) and space (selected eight points). Figure 11 shows the animation of piston's secondary motion in 500 r.p.m. motoring condition. This figure is exaggerated for clear visualization of piston's secondary motion, so we can observe the

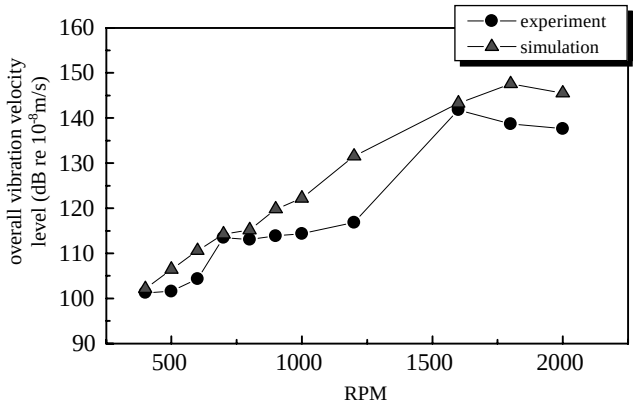

Figure 14. Comparison of estimated (△) and measured (○) overall vibration velocity level at engine block surface with respect to r.p.m.

rotaional motion and lateral motion in piston slap. In Figure 10, four small figures represent the impact force calculated by equations (10) and (11) using fourth-order Runge–Kutta method. Engine block surface vibration response is predicted by the convolution of calculated impact forces with 64 impulse responses, which is measured between eight cylinder inner walls (2 sides∗4 cylinders) and engine block surfaces (2 sides∗selected 4 points). Figure 12 is the schematic of experimental set-up in order to measure the vibration velocity level at engine block surfaces. A crankshaft is connected with a motor that drives the crankshaft of a commercial four-cylinder diesel engine with various speeds. The specifications of a commercial diesel engine are given in Appendix A.

Figure 13 shows the comparison between estimated and measured vibration velocity level at engine block surface in three selected motoring conditions. As shown in Figure 13, below 1/3 octave band center frequency 250 Hz, there is accoradance between simulation based on the proposed model and measured vibration velocity signal. But, above 1/3 octave band center frequency 500 Hz, there is somewhat large discordance between them. This is originated with the proposed model previously mentioned in section 2. This paper considers all collision points as equivalent vibratory systems that have the same mobility values as measured mobility with accordance below about 500 Hz. However, there is most vibration energy below 250 Hz. So, estimation of overall vibration level at engine block surface gives a similar tendency with experimental results as shown in Figure 14.

4. CONCLUSION

This paper proposes a simple model to estimate the impact forces induced by piston slap. In this work, piston skirt and cylinder inner wall are modelled on one-degree-of-freedom vibratory system which has the same (driving) point mobility. When slap occurs, the collision points are modelled on two-degree-of-freedom system, which is considered as a combination of one-degree-of-freedom vibratory systems of both piston skirt and cylinder inner wall. In order to verify the proposed model, numerical simulation based on the proposed model is compared with measured vibration response, which is obtained over a commercial engine block surface. The proposed collision point model can describe the behavior, that is point mobility, below about 500 Hz. On the other hand, there is some

discordance between predicted point mobility and the measured one above about 500 Hz. However, prediction of overall vibration level based on the proposed model shows similar tendency with measured vibration velocity level at engine block surface, because there exists most vibration energy below 1/3 octave band center frequency 250 Hz.

ACKNOWLEDGMENTS

This work was carried out as a part of National Research Laboratory (NRL) program financed by KISTEP (Korea Institute of Science and Technology Evaluation and Planning) and Brain Korea 21 (BK21) project initiated by Ministry of Education and Human Resources Development of Korea.

REFERENCES

1. E. E. UNGAR and D. ROSS 1965 *Journal of Sound and Vibration* **2**, 132–146. Vibration and noise due to piston slap in reciprocating machinery.
2. W. J. GRIFFITHS and J. SKORECKI 1964 *Journal of Sound and Vibration* **1**, 345–364. Some aspects of vibration of a single cylinder diegel engine.
3. N. LALOR, E. C. GROVER and T. PRIEDE 1980 SAE Paper 800402. Engine noise due to mechanical impacts at pistons and bearings.
4. J. W. SLACK 1984 *Ph.D. Dissertation*, *Department of Mechanical Engineering*, *Massachusetts Institute of Technology*. Piston slap in diesel engine.
5. R. WILSON and J. N. FAWCETT 1974 *Mechanism and Machine Theory* **9**, 61–80. Dynamics of the slider-crank mechanism with clearance in the sliding bearing.
6. F. FARAHANCHI and S. W. SHAW 1994 *Journal of Sound and Vibration* **177**, 307–324. Chaotic and periodic dynamics of a slider-crank mechanism with slider clearance.
7. K. OHTA, Y. IRIE, K. YAMAMOTO and H. ISHIKAWA 1987 1st *Report*, *Theoretical Analysis and Simulation*, *SAE Paper* 870990. Piston slap induced noise and vibration of internal combustion engines.
8. T. NAKADA, A. YAMAMOTO and T. ABE 1997 *SAE Paper* 972043. A numerical approach for piston secondary motion analysis and its application to the piston related noise.
9. D. J. EWINS 1986 *Modal Testing*: *Theory and Practice* pp. 153–159. Taunton: Research Studies Press Ltd.
10. L. E. KINSLER, A. R. FREY, A. B. COPPENS and J. V. SANDERS 1980, *Fundementals of Acoustics*, New York: John Wiley and Sons, Chapter 3.
11. J. D. FAIRES and R. L. BURDEN 1996 *Numerical Methods* pp. 208–216. International Thomson Publishing.

APPENDIX A

Dimensions of a commercial engine are given in Table A1.

TABLE A1

Piston	Cylinder	Crank-slider mechanism	Clearance
$m_p = 0{\cdot}8$ kg $I_p = 8$'*'10^{-4} kg m^2 $l_x = 0$ mm $l_y = 10$ mm	$R_B = 51{\cdot}05$ mm $x_{BO} = 0$ mm	$l = 0{\cdot}167$ m $r = 0{\cdot}05$ m	$c = 50$ μm

APPENDIX B

Parameters estimated by using equation (9) and experiment are given in Table B1.

TABLE B1

Piston skirt	Cylinder inner wall
$m_A = m_B = m_C = m_D = 0{\cdot}5$ kg	$\tilde{m}_A = \tilde{m}_B = \tilde{m}_C = \tilde{m}_D = 25$ kg
$k_A = k_B = k_C = k_D = 1{\cdot}4 * 10^7$ N/m	$\tilde{k}_A = \tilde{k}_B = \tilde{k}_C = \tilde{k}_D = 1{\cdot}9 * 10^8$ N/m
$c_A = c_B = c_B = c_D = 200$ N s/m	$\tilde{c}_A = \tilde{c}_B = \tilde{c}_C = \tilde{c}_D = 3000$ N s/m